

{Fe(NO)₂}⁹ Dinitrosyl Iron Complex Acting as a Vehicle for the NO Radical

Chun-Hung Ke,[†] Chien-Hong Chen,^{*,‡} Ming-Li Tsai,^{*,§} Hsuan-Chi Wang,[†] Fu-Te Tsai,[†]
Yun-Wei Chiang,[†] Wei-Chih Shih,[†] D. Scott Bohle,[#] and Wen-Feng Liaw^{*,†,‡,§}

[†]Department of Chemistry and Frontier Research Center of Fundamental and Applied Science of Matters, National Tsing Hua University, Hsinchu 30013, Taiwan

[‡]Department of Medical Applied Chemistry, Chung Shan Medical University, and Department of Medical Education, Chung Shan Medical University Hospital, Taichung 40201, Taiwan

[§]Department of Chemistry, National Sun Yat-sen University, Kaohsiung 80424, Taiwan

[#]Department of Chemistry, McGill University 801 Sherbrooke Street West, Montreal, Quebec H3A2K6, Canada

Supporting Information

ABSTRACT: To carry and deliver nitric oxide with a controlled redox state and rate is crucial for its pharmaceutical/medical applications. In this study, the capability of cationic {Fe(NO)₂}⁹ dinitrosyl iron complexes (DNICs) [(^RDDB)Fe(NO)₂]⁺ (R = Me, Et, Iso; ^RDDB = *N,N'*-bis(2,6-dialkylphenyl)-1,4-diaza-2,3-dimethyl-1,3-butadiene) carrying nearly unperturbed nitric oxide radical to form [(^RDDB)Fe(NO)₂(•NO)]⁺ was demonstrated and characterized by IR, UV-vis, EPR, NMR, and single-crystal X-ray diffractions. The unique triplet ground state of [(^RDDB)Fe(NO)₂(•NO)]⁺ results from the ferromagnetic coupling between two strictly orthogonal orbitals, one from Fe d_{z²} and the other a π*_{op} orbital of a unique bent axial NO ligand, which is responsible for the growth of a half-field transition (ΔM_S = 2) from 70 to 4 K in variable-temperature EPR measurements. Consistent with the NO radical character of coordinated axial NO ligand in complex [(^{Me}DDB)Fe(NO)₂(•NO)]⁺, the simple addition of MeCN/H₂O into CH₂Cl₂ solution of complexes [(^RDDB)Fe(NO)₂(•NO)]⁺ at 25 °C released NO as a neutral radical, as demonstrated by the formation of [S₃Fe(NO)₂]⁻ from [S₃Fe(μ-S)₂FeS₃]²⁻.

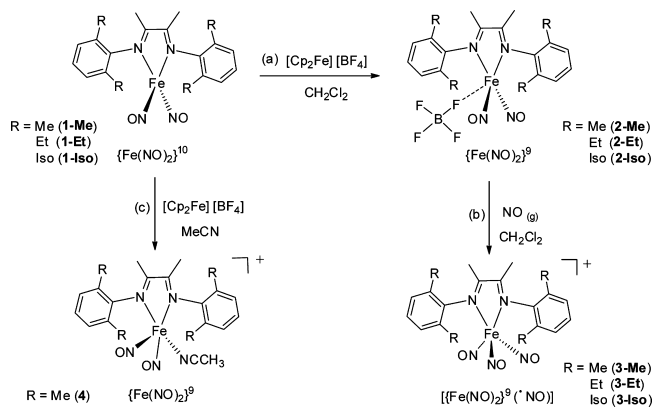
Driven by the versatile pharmaceutical/clinical applications of nitric oxide (NO) related to vasodilation, smooth muscle relaxation, inhibition of platelet aggregation, memory formation/learning processes in neurons, and cellular proliferation/differentiation/apoptosis,^{1,2} the fundamental investigations for storage and transport of highly reactive NO (with a physiological half-life <5 s) have attracted widespread interest in the past decades.² One of the key challenges of delivering NO for exerting physiological functions is to preserve the functionality of NO in complex biological environments before reaching the designated proteins/molecules.³ Although NOS isoforms are widely distributed, nature has evolved to utilize prevalent amino acid residues and abundant transition metal iron for storage and transport of NO in the forms of S-nitrosothiols (RSNOs) and dinitrosyl iron complexes (DNICs), respectively.^{4,5} Inspired by the diverse range of natural NO

carriers, researchers have tested an extensive series of NO-release compounds in preclinical studies/trials in order to modulate the relative stability as well as the releasing rates (e.g., SNP, GTN, PABA/NO, Spermine-NONOate, SNAP, DETA/NONOate, GSNO) (Table S1).^{6,7} Interestingly, DNICs present exceedingly diverse reactivities resulting from the non-innocent character of Fe-NO bonding interactions, such as S-nitrosylation, N-nitrosylation, nitrite/nitrate activation, H₂S storage, and the cellular permeation of DNICs/Roussin's red esters (RREs) for subsequent protein S-nitrosylation,^{8,9} also serving as pro-drugs capable of controlled delivery of NO to biological targets.¹⁰ Despite the diverse reactivities of DNICs which have been demonstrated,¹¹ the possibility/capability of {Fe(NO)₂} core serving as a vehicle to carry and deliver unperturbed NO radical is still unknown.¹² In this work, we synthesize and characterize NO-radical vehicle {Fe(NO)₂}⁹ DNICs [(^RDDB)Fe(NO)₂(•NO)][BF₄] (R = Me, Et, Iso; ^RDDB = *N,N'*-bis(2,6-dialkylphenyl)-1,4-diaza-2,3-dimethyl-1,3-butadiene) and control its release triggered by solvents (MeCN/H₂O).

Addition of 1 equiv of [Fe(CO)₂(NO)₂] to the THF solution of ^RDDB (R = Me, Et, Iso) led to the formation of four-coordinate {Fe(NO)₂}¹⁰ DNICs [(^{Me}DDB)Fe(NO)₂] (1-Me) ([(^{Et}DDB)Fe(NO)₂] (1-Et) and [(^{Iso}DDB)Fe(NO)₂] (1-Iso)) characterized by single-crystal X-ray diffractions (Figure S1).¹³ As shown in Scheme 1a and Figure S2, oxidation of {Fe(NO)₂}¹⁰ 1-Me by [Cp₂Fe][BF₄] in CH₂Cl₂ afforded the nonclassical five-coordinate {Fe(NO)₂}⁹ [(^{Me}DDB)Fe(NO)₂]-[BF₄] (2-Me) with the F atom of [BF₄]⁻ anion weakly coordinated to Fe metal (Fe...F = 2.28 Å), characterized by IR (ν_{NO} 1834 s, 1769 s cm⁻¹ (CH₂Cl₂)) and single-crystal X-ray diffraction (Figure S3). In a similar fashion, oxidation of {Fe(NO)₂}¹⁰ DNIC 1-Me by [Cp₂Fe][BF₄] in CH₃CN afforded the five-coordinate {Fe(NO)₂}⁹ [(^{Me}DDB)Fe(NO)₂(CH₃CN)][BF₄] (4) with CH₃CN coordinated to {Fe(NO)₂}⁹ core, characterized by IR (ν_{NO} 1801 s, 1724 s cm⁻¹ (CH₃CN)) and an EPR *g*-value (*g*_{av} = 2.019 at 77 K) (Scheme 1c),¹⁴ compared to the previous reports of Fe-based

Received: November 3, 2016

Scheme 1



oxidation of $\{\text{Fe}(\text{NO})_2\}^{10}$ [(sparteine) $\text{Fe}(\text{NO})_2$], yielding the unstable four-coordinate $\{\text{Fe}(\text{NO})_2\}^9$ [(sparteine) $\text{Fe}(\text{NO})_2$]- $[\text{BF}_4]$ with $\Delta\nu_{\text{NO}}$ shift 125 cm^{-1} and EPR $g_{\text{av}} = 2.032$.^{15,16}

Inspired by the formation of complex **4** with $\{\text{Fe}(\text{NO})_2\}^9$ core coordinated by α -diimine and CH_3CN , we injected dry NO (1.5-fold excess) into the CH_2Cl_2 solution of complex **2-Me** (complex **2-Et**) with a gastight syringe, as shown in Scheme 1b. The reaction solution was stirred under N_2 atmosphere at ambient temperature for 5 min. The color of the reaction solution changed from brown to dark green. The IR ν_{NO} stretching frequencies shifting from $(1834\text{ s}, 1769\text{ s})$ to $(1846\text{ s}, 1771\text{ vs}, 1753\text{ sh})\text{ cm}^{-1}$ indicate the formation of $[(^{\text{Me}}\text{DDB})\text{Fe}(\text{NO})_2(\cdot\text{NO})][\text{BF}_4]$ (**3-Me**) ($[(^{\text{Et}}\text{DDB})\text{Fe}(\text{NO})_2(\cdot\text{NO})][\text{BF}_4]$ (**3-Et**)), characterized by IR, UV-vis, EPR, NMR, and single-crystal X-ray diffraction (Figure 1).

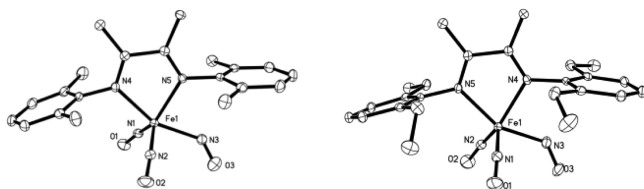
(a) Complex **3-Me**.(b) Complex **3-Et**.

Figure 1. ORTEP drawing and labeling scheme of $[(^{\text{R}}\text{DDB})\text{Fe}(\text{NO})_2(\cdot\text{NO})]^+$ ((a) $\text{R} = \text{Me}$ (**3-Me**), (b) $\text{R} = \text{Et}$ (**3-Et**)) with the thermal ellipsoid drawn at 50% probability. Hydrogen atoms are omitted for clarity. Selected bond lengths (\AA) and angles (deg): (a) $\text{Fe}(1)-\text{N}(1)$ 1.701(2), $\text{Fe}(1)-\text{N}(2)$ 1.676(2), $\text{Fe}(1)-\text{N}(3)$ 2.096(2), $\text{N}(1)-\text{O}(1)$ 1.159(2), $\text{N}(2)-\text{O}(2)$ 1.168(2), $\text{N}(3)-\text{O}(3)$ 1.141(2), $\text{Fe}(1)-\text{N}(1)-\text{O}(1)$ 164.3(1), $\text{Fe}(1)-\text{N}(2)-\text{O}(2)$ 169.9(2), $\text{Fe}(1)-\text{N}(3)-\text{O}(3)$ 120.1(1). (b) $\text{Fe}(1)-\text{N}(1)$ 1.683(2), $\text{Fe}(1)-\text{N}(2)$ 1.698(2), $\text{Fe}(1)-\text{N}(3)$ 2.062(2), $\text{N}(1)-\text{O}(1)$ 1.155(3), $\text{N}(2)-\text{O}(2)$ 1.158(3), $\text{N}(3)-\text{O}(3)$ 1.136(3), $\text{Fe}(1)-\text{N}(1)-\text{O}(1)$ 167.1(2), $\text{Fe}(1)-\text{N}(2)-\text{O}(2)$ 163.6(2), $\text{Fe}(1)-\text{N}(3)-\text{O}(3)$ 123.0(2).

In the same reaction condition, injection of NO into the CH_2Cl_2 solution of the more steric $^{\text{Iso}}\text{DDB}$ -containing analogue $[(^{\text{Iso}}\text{DDB})\text{Fe}(\text{NO})_2][\text{BF}_4]$ (**2-Iso**) displaying the IR ν_{NO} stretching frequencies at $1847\text{ s}, 1773\text{ vs}, 1742\text{ sh}\text{ cm}^{-1}$ suggested the formation of $[(^{\text{Iso}}\text{DDB})\text{Fe}(\text{NO})_2(\cdot\text{NO})][\text{BF}_4]$ (Figure S4). In contrast, addition of NO (1.5-fold excess) to $[(^{\text{Cyc}}\text{DDB})\text{Fe}(\text{NO})_2][\text{BF}_4]$ ($^{\text{Cyc}}\text{DDB} = \text{N,N}'\text{-dicyclohexylethylenediimine}$) (**2-Cyc**) did not yield the expected $[(^{\text{Cyc}}\text{DDB})\text{Fe}(\text{NO})_2(\cdot\text{NO})][\text{BF}_4]$. Presumably, it is mainly attributed to $^{\text{Cyc}}\text{DDB}$ promoting more electronic donation to the $\{\text{Fe}$

$(\text{NO})_2\}^9$ core hindering NO radical binding. Interestingly, upon CH_2Cl_2 solution of complex **3-Me** under vacuum at room temperature for 1 min, the IR ν_{NO} stretching frequencies shift from $(1846\text{ s}, 1771\text{ vs}, 1753\text{ sh}\text{ cm}^{-1})$ to $(1834\text{ s}, 1771\text{ s}\text{ cm}^{-1})$ via $(1846\text{ s}, 1834\text{ s}, 1771\text{ vs}, 1753\text{ sh}\text{ cm}^{-1})$ indicating the transformation of **3-Me** to **2-Me** under vacuum via the mixture of **3-Me** and **2-Me**, as shown in Figure S5 (a \rightarrow b \rightarrow c). The subsequent addition of NO gas into the CH_2Cl_2 solution of **2-Me** reformed complex **3-Me** (Figure S5 (c \rightarrow d)). These results suggest the IR ν_{NO} stretching frequency 1753 cm^{-1} (CH_2Cl_2) is mainly due to the "arrested" NO radical which is weakly bound and severely bent in the $\{\text{Fe}(\text{NO})_2\}^9$ core. Isotopic experiments (^{15}NO) led to the complete scrambling of the label. To further elucidate the NO-releasing ability of complexes **3-Me** and **3-Et**, addition of $\text{MeCN}/\text{H}_2\text{O}$ to the complexes **3-Me** (or **3-Et**) was conducted, respectively. Addition of 1 equiv of MeCN to CH_2Cl_2 solution of complex **3-Me** (5 mM) at $25\text{ }^\circ\text{C}$ yielded complex **4** (IR ν_{NO} stretching frequencies shifting from $(1846\text{ s}, 1771\text{ vs}, 1753\text{ sh})$ to $(1801\text{ s}, 1724\text{ s})\text{ cm}^{-1}$ (CH_2Cl_2)) accompanied by the release of NO, probed by $[\text{S}_3\text{Fe}(\mu\text{-S})_2\text{FeS}_5]^{2-}$ producing the known $[\text{S}_3\text{Fe}(\text{NO})_2]^-$.¹⁷ The half-life (32 min) of NO release was measured by UV-vis (based on absorption band 620 nm ($\epsilon = 202\text{ M}^{-1}\text{ cm}^{-1}$)) upon 1 equiv (or 2/4/10 equiv (SI Experimental Section)) of MeCN added into CH_2Cl_2 solution (5 mM) of complex **3-Me** at $25\text{ }^\circ\text{C}$ ($t_{1/2} = 42\text{ min}$ for addition of 1 equiv of H_2O into CH_2Cl_2 solution (5 mM) of complex **3-Me** at $25\text{ }^\circ\text{C}$).

Single-crystal X-ray structures of complexes **3-Me** and **3-Et** show the isostructural analogues (Figure 1). The average equatorial $\text{Fe}-\text{N}(\text{NO})$ bond distance of $1.688(2)\text{ \AA}$ ($\text{Fe}(1)-\text{N}(1)$ $1.701(2)\text{ \AA}$, and $\text{Fe}(1)-\text{N}(2)$ $1.676(2)\text{ \AA}$) and the average $\text{N}-\text{O}$ bond length of $1.163(2)\text{ \AA}$ ($\text{N}(1)-\text{O}(1)$ $1.159(2)\text{ \AA}$ and $\text{N}(2)-\text{O}(2)$ $1.168(2)\text{ \AA}$) observed in complex **3-Me** ($1.690(2)\text{ \AA}$ and $1.156(3)\text{ \AA}$ observed in complex **3-Et**, respectively) are consistent with those of other $\{\text{Fe}(\text{NO})_2\}^9$ DNICs.^{15,18} We notice the axial $\text{N}(3)-\text{O}(3)$ bond length of $1.141(2)\text{ \AA}$ for complex **3-Me** and $\text{N}(3)-\text{O}(3)$ bond length of $1.136(3)\text{ \AA}$ for complex **3-Et** are comparable to that (1.15 \AA) of free NO radical.¹⁹ The significantly longer axial $\text{Fe}(1)-\text{N}(3)$ bond length of $2.096(2)\text{ \AA}$ for **3-Me** and $\text{Fe}(1)-\text{N}(3)$ bond length of $2.062(2)\text{ \AA}$ for **3-Et**, in contrast to the average $\text{Fe}-\text{N}(\text{NO})$ bond distance falling in the range of $1.64\text{--}1.70\text{ \AA}$ for $\{\text{Fe}(\text{NO})_2\}^9$ DNICs,¹⁸ implicate the axial $\text{N}(3)\text{O}(3)$ radical is "arrested" by the $\{\text{Fe}(\text{NO})_2\}^9$ core. It is noted that the diamagnetic $\{\text{Fe}(\text{NO})_3\}^{10}$ trinitrosyl iron complex (TNIC) $[(\text{Imes})\text{Fe}(\text{NO})_3][\text{BF}_4]$ bound by three nearly equivalent NO ligands with average $\text{N}-\text{O}$ bond distance of $1.143(6)\text{ \AA}$ and average $\text{Fe}-\text{N}(\text{NO})$ bond distance of $1.688(5)\text{ \AA}$ were reported by Darensbourg and other groups.¹² Of importance, in contrast to the average $\text{Fe}-\text{N}-\text{O}$ bond angle of 173.5° obtained in TNIC,¹² the $\text{Fe}(1)-\text{N}(3)-\text{O}(3)$ bond angle of 120.1° in complex **3-Me** and $\text{Fe}(1)-\text{N}(3)-\text{O}(3)$ bond angle of 123.0° in complex **3-Et** were observed.

In contrast to the diamagnetic $\{\text{Fe}(\text{NO})_3\}^{10}$ TNIC,¹² EPR spectrum of complex **3-Me** exhibits a rhombic signal $g_{\text{av}} = 2.019$ and a weak half-field signal at $g = 3.99$ at 77 K (Figure 2). The formally forbidden transition due to $\Delta M_s = 2$ is detected at approximately 1700 G , consistent with the expected transition. The intensity of the half-field resonance increases with decreasing temperature (Figure 2b), in line with the typical temperature-dependent changes of EPR signal intensity for a molecule with triplet ground state.²⁰ Presumably, the weak magnetic coupling (dipolar coupling) between the $\{\text{Fe}$

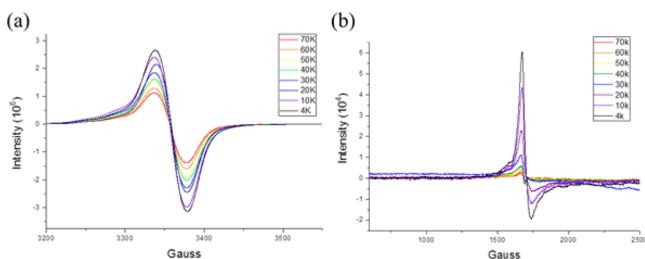


Figure 2. Variable-temperature EPR spectra of complex **3-Me**: (a) $g_{av} = 2.019$ ($g_1 = 2.036$, $g_2 = 2.019$, $g_3 = 2.004$) from 70 to 4 K and (b) the half-field signal at $g = 3.99$ from 70 to 4 K in CH_2Cl_2 .

$(\text{NO})_2\}^9$ center ($S = 1/2$) and NO radical ($S = 1/2$) of complex **3-Me** rationalizes the weak ferromagnetic coupling, leading to triplet ground state also supported by the magnetic moment of $\mu_{\text{eff}} = 2.085 \mu_B$ obtained from Evans's method at 183 K.²¹ At low temperatures, the zero-field splitting of the resonance is observed and value of $D \approx 0.0022 \text{ cm}^{-1}$ and $g_{av} = 2.019$ are obtained based on a triplet-state low-temperature EPR theoretical analysis using EasySpin²² (Figure S6). Furthermore, the J value is determined as $(0.58 \pm 0.05) \text{ cm}^{-1}$ from theoretical fitting of intensity variation of EPR signal as a function of temperatures,²⁰ as shown in Figure S7.

DFT calculations were performed to gain an insight into the electronic structure and bonding interactions of **3-Me** as well as rationalize the unusual long axial Fe–N(NO) bond distance.^{11,18} The DFT structure was further verified spectroscopically by the spin-Hamiltonian parameters derived from the experimental EPR spectra (as detailed in Figure 2) and IR ν_{NO} stretching frequencies.²⁴ Although the calculated IR ν_{NO} stretching frequencies ($1893, 1805, 1793 \text{ cm}^{-1}$) are slightly overestimated by $\sim 40 \text{ cm}^{-1}$, the characteristic small separation between first two ν_{NO} stretching frequencies ($\Delta\nu_{\text{NO}}^1(\text{exp}) = 18 \text{ cm}^{-1}$, $\Delta\nu_{\text{NO}}^1(\text{calc}) = 13 \text{ cm}^{-1}$) and big separation between the last two ν_{NO} stretching frequencies ($\Delta\nu_{\text{NO}}^2(\text{exp}) = 75 \text{ cm}^{-1}$, $\Delta\nu_{\text{NO}}^2(\text{calc}) = 88 \text{ cm}^{-1}$) are successfully reproduced. The spin density distribution shown in Figure 3a clearly indicates the antiferromagnetic coupling interactions between Fe center and two equatorial NO ligands evidenced by positive and negative spin density on the Fe center and two equatorial NO ligands, respectively.

In addition, the orbital energy diagram and population analysis of key orbitals associated with Fe and equatorial NO ligands (Figure S8) also support the description of electronic structure of $(\text{MeDDB})\text{Fe}(\text{NO})_2$ fragment in **3-Me** as $\{\text{Fe}^{\text{III}}(\text{NO}^-)_2\}^9$, which is consistent with previous DFT computational²³ and valence-to-core X-ray emission spectroscopic studies.²⁴ On the other hand, the axial NO ligand possess positive spin density ($\rho_{\text{NO}(\text{axial})} \approx 1.15$) and predominantly localized on π^*_{op} orbital. The orthogonality between the Fe d_{z^2} orbital of $(\text{MeDDB})\text{Fe}(\text{NO})_2$ fragment and π^*_{op} orbital of coordinated axial NO ligand (Figure 3b) derived from the analysis of bonding molecular orbitals $\alpha 110$ and $\alpha 115$ (Figure S8) provides a plausible pathway for a ferromagnetic coupling interaction and the orbital rationales for the observation characteristic EPR half-field transition indicating triplet ground state of **3-Me**. The normal modes of three ν_{NO} stretching frequencies observed in the CH_2Cl_2 solution of complex **3-Me** are tentatively assigned from the DFT vibrational calculations (Figure 3c). Consistent with the preceding assignment, the 1753 cm^{-1} IR vibrational mode is composed of major axial NO stretching coupled with a minor

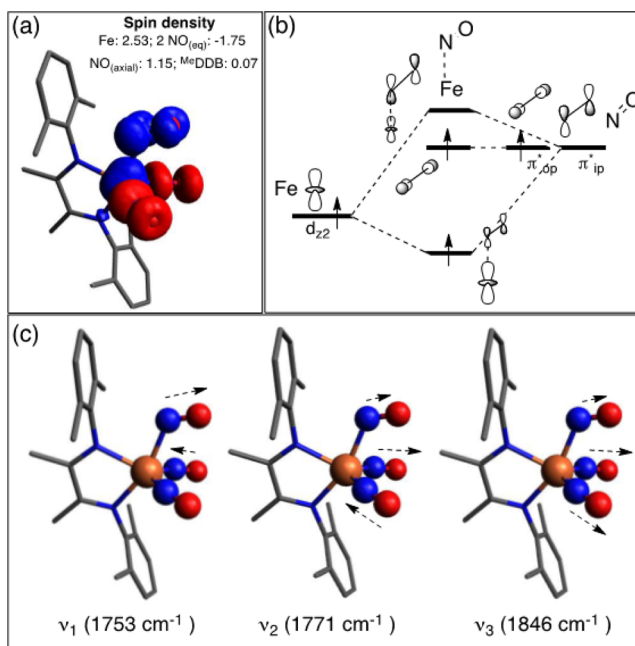


Figure 3. Bonding and vibrational analysis obtained from DFT calculations of **3-Me**. (a) Spin density distribution of DFT-optimized **3-Me**. (b) Representative bonding interactions between $\{\text{Fe}(\text{NO})_2\}^9$ core and axial NO of **3-Me**. The labels “ip” and “op” of axial $\text{NO}\pi^*$ orbitals refer to “in-plane” and “out-of-plane”, respectively; the planes for the notations are defined by axial Fe–N–O. (c) Pictorial representation of three normal modes associated with axial and equatorial ν_{NO} stretching vibrations derived from DFT calculations.

contribution from one of the equatorial NO ligands. The 1771 and 1846 cm^{-1} IR vibrational modes are best described as well-characterized asymmetric and symmetric vibrational modes of two equatorial NO ligands of DNICs, respectively, where both vibrational modes mix with a minor contribution from axial ν_{NO} stretching.

In conclusion, we have successfully demonstrated that $\{\text{Fe}(\text{NO})_2\}^9$ DNICs is capable of acting as a NO radical vehicle and are easily prepared by reacting $\text{NO}_{(\text{g})}$ with cationic $\{\text{Fe}(\text{NO})_2\}^9$ [$(\text{R}^{\text{DDB}})\text{Fe}(\text{NO})_2$]⁺. In contrast to the reported TNICs,¹² the [$(\text{R}^{\text{DDB}})\text{Fe}(\text{NO})_2(\text{*NO})$]⁺ exhibits an unusual long Fe–N(NO) (axial) bond distance ($\sim 2.096 \text{ \AA}$) as well as unprecedented triplet ground state resulting from ferromagnetic coupling between two orthogonal orbitals (Fe d_{z^2} orbital and π^*_{op} orbital of axial NO ligand). The unique geometry and electronic structure facilitates a fast NO radical release triggered by simply adding MeCN/ H_2O to replace the weakly coordinating axial NO ligand without compromising the structural integrity of $\{\text{Fe}(\text{NO})_2\}^9$ [$(\text{R}^{\text{DDB}})\text{Fe}(\text{NO})_2$]⁺ vehicle. A combination of well-established strategies of the targeted drug delivery (liposome, micelle, biodegradable polymers/particles, etc.) and the exceptional ability of $\{\text{Fe}(\text{NO})_2\}^9$ motif for storage and release NO radical could be promising directions for treating cardiovascular disease and malignant tumors.

■ ASSOCIATED CONTENT

📄 Supporting Information

The Supporting Information is available free of charge on the ACS Publications website at DOI: 10.1021/jacs.6b11454.

Experimental details, Tables S1–S3, and Figures S1–S8 (PDF)

X-ray crystallographic files for structure determinations of [(^{Me}DDB)Fe(NO)₂([•]NO)][BF₄], [(^{Et}DDB)Fe(NO)₂([•]NO)][BF₄], [(^{Me}DDB)Fe(NO)₂][BF₄], [(^{Is}DDB)Fe(NO)₂][BF₄], [(^{Me}DDB)Fe(NO)₂], [(^{Et}DDB)Fe(NO)₂], and [(^{Is}DDB)Fe(NO)₂](ClF)

AUTHOR INFORMATION

Corresponding Authors

*wfliaw@mx.nthu.edu.tw
*mltsai@mail.nsysu.edu.tw
*cchwind@csmu.edu.tw (CHC)

ORCID

Yun-Wei Chiang: 0000-0002-2101-8918

Wen-Feng Liaw: 0000-0001-9949-8344

Notes

The authors declare no competing financial interest.

ACKNOWLEDGMENTS

We gratefully acknowledge financial support from the Ministry of Science & Technology of Taiwan. The authors thank Dr. Chang-Chih Hsieh, Miss Pei-Lin Chen, and Mr. Ting-Shen Kuo for single-crystal X-ray structural determinations. We also thank NCHC for their support on the software applied in this work.

REFERENCES

- (1) (a) Pacher, P.; Beckman, J. S.; Liaudet, L. *Physiol. Rev.* **2007**, *87*, 315–424. (b) Szacilowski, K.; Chmura, A.; Stasicka, Z. *Coord. Chem. Rev.* **2005**, *249*, 2408–2436.
- (2) Ignarro, L. J.; Buga, G. M.; Wood, K. S.; Byrns, R. E.; Chaudhuri, G. *Proc. Natl. Acad. Sci. U. S. A.* **1987**, *84*, 9265–9269.
- (3) (a) Butler, A. R.; Megson, I. L. *Chem. Rev.* **2002**, *102*, 1155–1165. (b) Chen, Y.-J.; Ku, W.-C.; Feng, L.-Ti; Tsai, M.-L.; Hsieh, C.-H.; Hsu, W.-H.; Liaw, W.-F.; Hung, C.-H.; Chen, Y.-J. *J. Am. Chem. Soc.* **2008**, *130*, 10929–10938.
- (4) (a) Wang, P. G.; Xian, M.; Tang, X.; Wu, X.; Wen, Z.; Cai, T.; Janczuk, A. J. *Chem. Rev.* **2002**, *102*, 1091–1134. (b) Lee, J.; Chen, L.; West, A. H.; Richter-Addo, G. B. *Chem. Rev.* **2002**, *102*, 1019–1065.
- (5) (a) Bosworth, C. A.; Toledo, J. C., Jr.; Zmijewski, J. W.; Li, Q.; Lancaster, J. R., Jr. *Proc. Natl. Acad. Sci. U. S. A.* **2009**, *106*, 4671–4676. (b) Tsou, C.-C.; Liaw, W.-F. *Chem. - Eur. J.* **2011**, *17*, 13358–13366.
- (6) (a) Terwel, D.; Nieland, L. J. M.; Schutte, B.; Reutelingsperger, C. P. M.; Ramaekers, F. C. S.; Steinbusch, H. W. M. *Eur. J. Pharmacol.* **2000**, *400*, 19–33. (b) Kumar, V.; Hong, S. Y.; Maciag, A. E.; Saavedra, J. E.; Adamson, D. H.; Prud'homme, R. K.; Keefer, L. K.; Chakrapani, H. *Mol. Pharmaceutics* **2010**, *7*, 291–298.
- (7) (a) Mohr, S.; Stampler, J. S.; Brune, B. *FEBS Lett.* **1994**, *348*, 223–227. (b) Mocellin, S.; Bronte, V.; Nitti, D. *Med. Res. Rev.* **2007**, *27*, 317–352.
- (8) (a) Tsou, C.-C.; Chiu, W.-C.; Ke, C.-H.; Tsai, J.-C.; Wang, Y.-M.; Chiang, M.-H.; Liaw, W.-F. *J. Am. Chem. Soc.* **2014**, *136*, 9424–9433. (b) Tsai, F.-T.; Chen, P.-L.; Liaw, W.-F. *J. Am. Chem. Soc.* **2010**, *132*, 5290–5299.
- (9) (a) Tinberg, H. E.; Tonzetich, Z. J.; Wang, H.; Do, L. H.; Yoda, Y.; Cramer, S. P.; Lippard, S. J. *J. Am. Chem. Soc.* **2010**, *132*, 18168–18176. (b) Filipovic, M. R.; Miljkovic, J. L.; Nausier, T.; Royzen, M.; Klos, K.; Shubina, T.; Koppenol, W. H.; Lippard, S. J.; Ivanović-Burmazović, I. *J. Am. Chem. Soc.* **2012**, *134*, 12016–12027. (c) Tran, C. T.; Williard, P. G.; Kim, E. J. *J. Am. Chem. Soc.* **2014**, *136*, 11874–11877.
- (10) Wu, S.-C.; Lu, C.-Y.; Chen, Y.-L.; Lo, F.-C.; Wang, T.-Y.; Chen, Y.-J.; Yuan, S.-S.; Liaw, W.-F.; Wang, Y.-M. *Inorg. Chem.* **2016**, *55*, 9383–9392.
- (11) (a) Pulukkody, R.; Darensbourg, M. Y. *Acc. Chem. Res.* **2015**, *48*, 2049–2058. (b) Tsai, M.-L.; Tsou, C.-C.; Liaw, W.-F. *Acc. Chem. Res.* **2015**, *48*, 1184–1193.
- (12) (a) Hsieh, C.-H.; Darensbourg, M. Y. *J. Am. Chem. Soc.* **2010**, *132*, 14118–14125. (b) Dillinger, S. A. T.; Schmalle, H. W.; Fox, T.; Berke, H. *J. Chem. Soc., Dalton Trans.* **2007**, 3562–3571. (c) Beck, W.; Klapotke, T. M.; Mayer, P. Z. *Anorg. Allg. Chem.* **2006**, *632*, 417–420. (d) Hayton, T. W.; McNeil, W. S.; Patrick, B. O.; Legzdins, P. *J. Am. Chem. Soc.* **2003**, *125*, 12935–112944.
- (13) Reginato, N.; McCrory, C. T. C.; Pervitsky, D.; Li, L. *J. Am. Chem. Soc.* **1999**, *121*, 10217–10218.
- (14) Shih, W.-C.; Lu, T.-T.; Yang, L.-B.; Tsai, F.-T.; Chiang, M.-H.; Lee, J.-F.; Chiang, Y.-W.; Liaw, W.-F. *J. Inorg. Biochem.* **2012**, *113*, 83–93.
- (15) Hung, M.-C.; Tsai, M.-C.; Lee, G.-H.; Liaw, W.-F. *Inorg. Chem.* **2006**, *45*, 6041–6047.
- (16) Chen, C.-H.; Ho, Y.-C.; Lee, G.-H. *J. Organomet. Chem.* **2009**, *694*, 3395–3400.
- (17) Tsai, M.-L.; Chen, C.-C.; Hsu, I.-J.; Ke, S.-C.; Hsieh, C.-H.; Chiang, K.-A.; Lee, G.-H.; Wang, Y.; Chen, J.-M.; Lee, J.-F.; Liaw, W.-F. *Inorg. Chem.* **2004**, *43*, 5159–5167.
- (18) Tsou, C.-C.; Tsai, F.-T.; Chen, H.-Y.; Hsu, I.-J.; Liaw, W.-F. *Inorg. Chem.* **2013**, *52*, 1631–1639.
- (19) McCleverty, J. A. *Chem. Rev.* **2004**, *104*, 403–418.
- (20) (a) Abe, M. *Chem. Rev.* **2013**, *113*, 7011–7088. (b) Lu, C. C.; Bill, E.; Weyhermüller, T.; Bothe, E.; Wieghardt, K. *J. Am. Chem. Soc.* **2008**, *130*, 3181–3197. (c) Eaton, S. S.; More, K. M.; Sawant, B. M.; Eaton, G. R. *J. Am. Chem. Soc.* **1983**, *105*, 6560–6567. (d) Blumberg, W. E.; Peisach, J. *Ann. N. Y. Acad. Sci.* **1973**, *222*, 539–560.
- (21) (a) Evans, D. F. *J. Chem. Soc.* **1959**, 2003–2005. (b) Löliger, J.; Scheffold, R. *J. Chem. Educ.* **1972**, *49*, 646–647.
- (22) Stoll, S.; Schweiger, A. *J. Magn. Reson.* **2006**, *178*, 42–55.
- (23) (a) Tsai, M.-C.; Tsai, F.-T.; Lu, T.-T.; Tsai, M.-L.; Wei, Y.-C.; Hsu, I. J.; Lee, J.-F.; Liaw, W.-F. *Inorg. Chem.* **2009**, *48*, 9579–9591. (b) Ye, S.; Neese, F. *J. Am. Chem. Soc.* **2010**, *132*, 3646–3647.
- (24) Lu, T.-T.; Weng, T.-C.; Liaw, W.-F. *Angew. Chem., Int. Ed.* **2014**, *53*, 11562–11566.